THE ASTROPHYSICAL JOURNAL, 460:L111–L114, 1996 April 1
© 1996. The American Astronomical Society. All rights reserved. Printed in U.S.A.

A POSSIBLE MECHANISM FOR WIGGLING PROTOSTELLAR JETS FROM THREE-DIMENSIONAL SIMULATIONS IN A STRATIFIED AMBIENT MEDIUM

ELISABETE M. DE GOUVEIA DAL PINO,[1] MARK BIRKINSHAW,[2,3] AND WILLY BENZ[4]
Received 1995 April 17; accepted 1996 January 25

ABSTRACT

Most collimated supersonic protostellar jets show a collimated wiggling, and knotty structure (e.g., the Haro 6-5B jet) and frequently reveal a long gap between this structure and the terminal bow shock. In a few cases, there is no evidence of such a terminal feature. We present three-dimensional smoothed particle hydrodynamical simulations that suggest that this morphology may be due to the interaction of the propagating cooling jet with a nonhomogeneous ambient medium. In regions where the ambient gas has an increasing density (and pressure) gradient, we find that it tends to compress the cold, low-pressure cocoon of shocked material that surrounds the beam, destroy the bow shock–like structure at the head, and enhance beam focusing, wiggling, and internal traveling shocks. In ambient regions of decreasing density (and pressure), the flow widens and relaxes, becoming very faint. This could explain "invisible" segments in systems like the Haro 6-5B jet. The bow shock in these cases could be a relic of an earlier outflow episode, as previously suggested, or the place where the jet reappears after striking a denser portion of the ambient medium.

Subject headings: hydrodynamics — ISM: jets and outflows — stars: mass loss — stars: pre–main-sequence

1. INTRODUCTION

Protostellar jets propagate into a complex ambient medium. They are immersed in molecular clouds that are generally inhomogeneous and formed of many small, dense clouds that are sites of star formation (see, e.g., Bally & Devine 1994). Previous three-dimensional numerical modeling of continuous and intermittent jets emanating from protostars were performed with beams propagating into homogeneous ambient media (see, e.g., de Gouveia Dal Pino & Benz 1993, 1994, hereafter GB93, GB94; Chernin et al. 1994; hereafter CMGB; Stone & Norman 1994). These simulations have reproduced the basic features typically observed in protostellar jets: the chain of more or less regularly spaced knots along the beam, produced mainly in jets with intermittent ejection; or the formation of bow shock–like structures at the jet head, with a dense shell composed of filaments and blobs developed from Rayleigh-Taylor and global thermal instabilities. We here report three-dimensional numerical results for jets propagating through ambient gas with power-law density (and pressure) distributions and examine their effects on the structure of the jets.

In recent work, concerned with environmental effects on extragalactic jets, Wiita, Rosen, & Norman (1990) and Hardee et al. (1992) have performed two-dimensional hydrodynamical simulations of adiabatic, light jets propagating into a stratified intergalactic medium. In contrast to such extragalactic flows, the cooling distance of postshock protostellar jet gas is smaller than the jet radius and hence the assumption of an adiabatic gas is inappropriate. We here analyze the effects of a stratified ambient medium on radiatively cooling, initially heavy (denser than their surroundings) jets—a picture generally believed to be more appropriate to protostellar jets (see, e.g., Mundt et al. 1990). A more detailed description of the results of this investigation, with simulations covering a more extensive range of parameters, is presented elsewhere (de Gouveia Dal Pino & Birkinshaw 1996, hereafter GB96).

2. NUMERICAL METHOD

We solve the hydrodynamics equations using a modified version of the three-dimensional Cartesian, gridless, Lagrangian smoothed particle hydrodynamics (SPH) code described in GB93, GB94, CMGB, and GB96. The ambient gas is represented by a three-dimensional rectangular box filled with particles. A collimated, supersonic jet of radius R_j is continuously injected into the bottom of the box, which has dimensions of $\simeq 20\ R_j$ in the x-axis and $12\ R_j$ in the transverse directions (y and z). The boundaries of the box are assumed to be continuous. The SPH particles are smoothed by a spherically symmetric kernel function of width h. The initial values of h were chosen to be $0.5\ R_j$ and $0.25\ R_j$ for the ambient and jet particles, respectively. The jet and the ambient gas are treated as a single ionized fluid with an ideal gas equation of state and a ratio of specific heats $\gamma = 5/3$. Radiative cooling (due to collisional excitation and recombination) is implicitly calculated using the local, time-independent cooling function for a gas of cosmic abundances cooling from $T \simeq 10^6$–10^4 K (Katz 1989).

We assume an initial isothermal ambient medium ($T_a = 10^4$ K) with density (and pressure) distribution stratified along the jet axis,

$$n_a(x) = n_a(x_0)[\alpha(x - x_0) + 1]^{\beta}, \qquad (1)$$

where n_a is the ambient number density, x_0 is the value of x at the jet inlet (in units of the jet radius R_j), α is a parameter of the model, and the exponent $\beta = \pm 5/3$ for positive and negative density gradients, respectively. Such profiles are consistent with the observed density distributions of clouds which involve protostars (see, e.g., Fuller & Myers 1992). A

[1] Instituto Astronômico e Geofísico, Universidade de São Paulo, Av. Miguel Stéfano 4200 (04301-904), São Paulo SP, Brazil; dalpino@astro1.iagusp.usp.br.
[2] Center for Astrophysics, 60 Garden Street, Cambridge, MA, 02178.
[3] Present address: University of Bristol, Department of Physics, Bristol, UK.
[4] University of Arizona, Steward Observatory and Lunar and Planetary Laboratory, Tucson, AZ 85721.

negative density gradient may represent, for example, the atmosphere that a jet encounters as it propagates through a portion of the cloud that envelops the parent source. A positive density gradient will occur when a jet enters an external cloud. In the simulations the atmosphere was held steady by an appropriate gravitational potential.

A supersonic jet propagating into a stationary ambient gas will develop a shock pattern at its head, where the impacted ambient material is accelerated by a forward bow shock and the jet material is decelerated at the jet shock. Our models of hydrodynamical jets are characterized by dimensionless parameters $\eta = n_j(x_0)/n_a(x_0)$, the ratio between the jet and ambient number densities at x_0; $M_a = v_j/c_a$ the ambient Mach number, where v_j is the jet injection velocity and c_a is the sound speed in the ambient material; and $q_{\rm bs} = d_{\rm cool}/R_j$, the ratio of the cooling length in the postshock gas behind the bow shock to the jet radius (which, for shock velocities >90 km s^{-1}, is related to the ratio measured in the postshock gas behind the jet shock, $q_{\rm js}$, via $q_{\rm js} \simeq q_{\rm bs}\eta^{-3}$ (cf., GB93). The parameters of the simulations were chosen to resemble the conditions found in protostellar jets. Based on observations, we adopt the values $\eta = 1$–10; $v_j \simeq 400$ km s^{-1}; $M_a = 24$, and $R_j = 2 \times 10^{15}$ cm. We assume $\alpha = 0.5$ and $\beta = \pm 5/3$ in equation (1). (See GB96 for a wider range of parameters.)

3. THE SIMULATIONS

Figure 1 depicts the central density contours of three distinct jets when they have propagated a distance $\simeq 20\, R_j$. All flows were initially in pressure equilibrium at the jet inlet, with $\eta(x_0) = 3$, $n_a(x_0) = 200$ cm^{-3}, $R_j = 2 \times 10^{15}$ cm, $v_j = 398$ km s^{-1}, $M_a = 24$, $q_{\rm bs} \simeq 8.1$, $q_{\rm js} \simeq 0.3$, and $R_j/c_a = 38.2$ yr. In Figure 1*a* the ambient medium has positive density gradient ($\beta = 5/3$, $\alpha = 0.5$); in Figure 1*b* it is homogeneous, and in Figure 1*c* it has negative density gradient ($\beta = -5/3$, $\alpha = 0.5$). The cooling length parameters imply that the ambient shocked gas is initially almost adiabatic whereas the shocked jet material is highly radiative (see, e.g., Blondin, Fryxell, & Königl 1990, hereafter BFK; GB93). The jets reach the end of the computation domain at (in units of R_j/c_a): Figure 1*a*, $t = 1.65$; Figure 1*b*, $t = 1.15$; and Figure 1*c*, $t = 0.95$. In the homogeneous medium case (Fig. 1*b*), we can identify the same basic features detected in previous work (see, e.g., GB93; GB94; CMGB). The working surface, at the head of the jet, develops a dense shell (with density $n_{\rm sh} \sim 469 n_a$) of shocked jet material that becomes Rayleigh-Taylor unstable (GB93) and breaks into blobs. A low-density cocoon containing postshock jet gas is deposited around the jet beam. A dense shroud of shocked ambient gas envelops both the beam and the cocoon.

In the increasing density medium (Fig. 1*a*), the cocoon is compressed and pushed backward by the increasing ram pressure of the ambient gas. The bow-shock shape seen at the head of the jet propagating into a uniform medium (Fig. 1*b*) is replaced in Figure 1*a* by an elongated structure, and the beam and shell [$n_{\rm sh}/n_a(x_0) \simeq 783$] are highly focused. The high pressure of the surrounding medium promotes Kelvin-Helmholtz instabilities (see, e.g., Birkinshaw 1991) with the excitation of pinch and helical modes which collimate the beam, drive internal shocks, and cause some jet twisting and flapping. A similar structure has been found for adiabatic jets propagating into a homogeneous ambient medium (see, e.g., GB93), but there the collimation of the jet is a result of the hot, high-pressure, postshock jet gas in the cocoon immediately behind the working surface (cf., BFK, GB93). The internal shocks in the beam have a typical separation of few jet diameters, in agreement with observations of internal knots in protostellar jets.

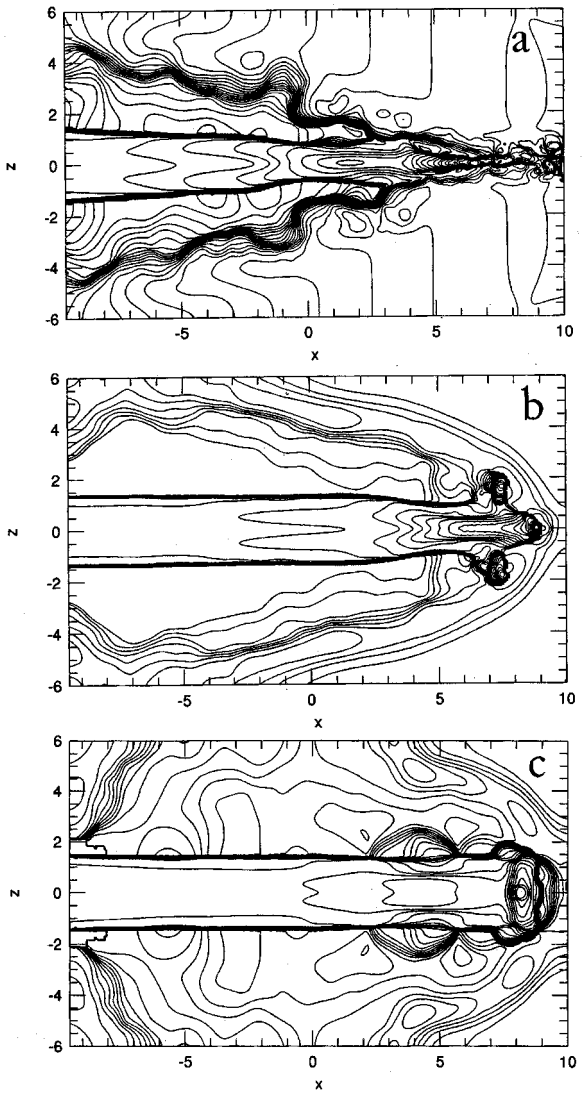

FIG. 1.—Central density contours of jets with $\eta(x_0) = 3$ and $M_a = 24$. In (*a*) the ambient medium has positive density gradient ($\beta = 5/3$, $\alpha = 0.5$), in (*b*) it is homogeneous, and in (*c*) it has negative density gradient ($\beta = -5/3$, $\alpha = 0.5$). The coordinates x and z are in units of R_j. The contour lines are separated by a factor of 1.3, and the peak of the density scale is $800/n_a(x_0)$.

In the decreasing density medium (Fig. 1*c*) the cocoon that surrounds the beam becomes broad and relaxed, the jet shows no internal shocks, and we clearly see an acceleration of the jet as it propagates due to the decreasing ambient density and ram pressure. Compared to the jet propagating into the homogeneous medium (Fig. 1*b*), the beam is much less collimated close to the head. An analysis of the density and velocity maps indicates a ratio of the jet-to-head radius $\epsilon^{1/2} \equiv R_j/R_h \simeq 0.8$. This decollimation is significantly larger for lower-density jets (GB96). The cold shell at the working surface is thin, does not fragment, and has a smaller overdensity [$n_{\rm sh}/n_a(x_0) \simeq 33$] than the jet propagating into the homogeneous ambient medium, which indicates the faintness of radiative shocks at the head. For an ambient medium with negative density gradient, the

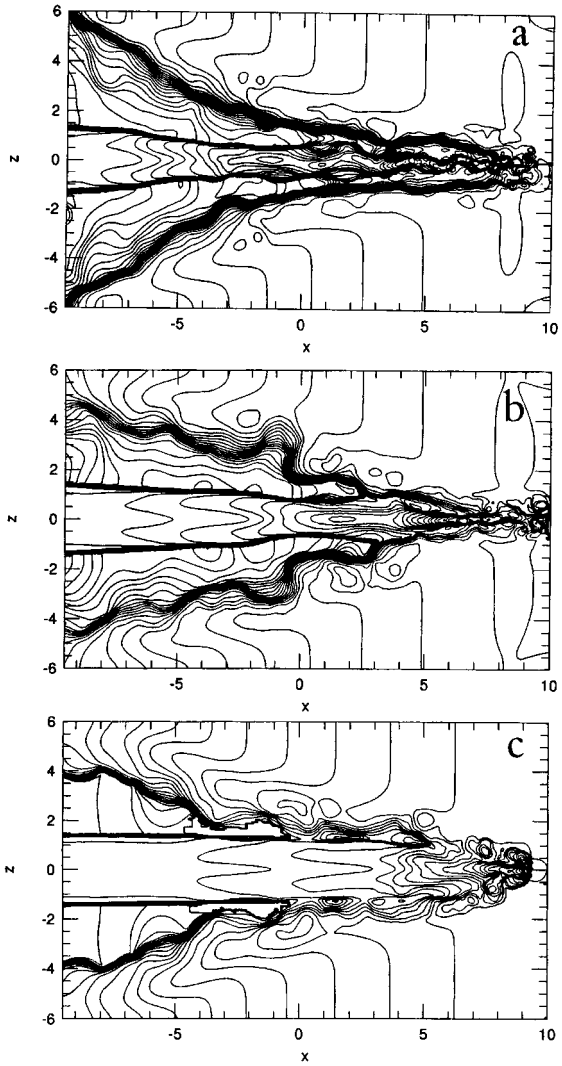

FIG. 2.—Jets with distinct $\eta(x_0)$ in an $\alpha = 0.5$ ambient medium with positive stratification. (*a*) $\eta(x_0) = 1$, (*b*) $\eta(x_0) = 3$, and (*c*) $\eta(x_0) = 10$. The initial conditions are the same as in Fig. 1. The maximum density of the shells at the jet heads are $n_{sh}/n_a(x_0) \simeq 211$ (*a*), 638 (*b*), and 2540 (*c*).

cooling length behind the bow shock (q_{bs}) should increase as the jet propagates downstream and the cooling length behind the jet shock should decrease (see, e.g., GB93; GB96). Thus the bow shock becomes more adiabatic as the beam propagates, while the jet shock becomes more radiative but fainter since the jet shock velocity, $v_{js} \simeq v_j - v_{ws}$, decreases as the bow-shock speed v_{ws} increases. The opposite is true in the case of the ambient medium with positive density gradient.

Figure 2 depicts jets with different values of η propagating into an $\alpha = 0.5$ ambient medium with positive ($\beta = 5/3$) density (and pressure) stratification. The jets reach the end of the compution domain at (in units of R_j/c_a): Figure 2*a*, $t = 1.85$; Figure 2*b*, $t = 1.65$; and Figure 2*c*, $t = 1.25$. The highest density jet reaches the end of the domain earlier and is least affected by the increasing ambient density and pressure gradients.

4. DISCUSSION AND CONCLUSIONS

What do these results have to do with the observed protostellar jets? Our simulations show that jets propagating into portions of an ambient medium with negative density (pressure) gradient develop a broad and relaxed cocoon and the beam rapidly accelerates due to the drop of the ambient density and ram pressure. No internal knots are formed in this case and the radiative shocks at the head are faint and will provide little radiation (Fig. 1*c*). This is consistent with the "invisible" portions of the observed outflows, e.g., the gaps close to the source of Haro 6-5B (FS Tau B) (Mundt, Ray, & Raga 1991, hereafter MRR), AS 353A (see, e.g., Hartigan, Mundt, & Stocke 1986), and 1548 C27 (see, e.g., Mundt, Brugel, & Bührke 1987). On the other hand, jets propagating into portions of an ambient medium with increasing density (pressure) have their cocoon/shroud compressed and pushed backward by the ambient ram pressure and the beam is highly collimated. The compressing medium promotes Kelvin-Helmholtz (K-H) instabilities that cause beam pinching, twisting, and flapping (Figs. 1*a* and 2). This favors the formation of regularly spaced, traveling, internal knots and an increase in the jet confinement, as required by observations, but the bow shocklike structure at the head disappears.

Observed jets are, in general, well collimated and knotty and many show one or more bright bow shock–like structures at the head (see, e.g., Reipurth 1989). In GB94 (see also, e.g., Hartigan & Raymond 1992; Raga & Kofman 1992; Stone & Norman 1993; Massaglia et al. 1995), we showed that the internal traveling knots can be a product of rapid variations in the jet ejection speed. We also have demonstrated that bow shocks can be formed in jets with continuous ejection (GB93) or with multiple outflow episodes of long period (GB94) and can keep their structure approximately stable in portions of the jet where the ambient medium is more homogeneous (GB93). There are, however, some observed jets whose visible structures resemble remarkably the simulated jets of Figure 2, which propagate into ambient gas with increasing density gradient, as for example, Haro 6-5B-northern and HH 24G jets (see, e.g., Mundt et al. 1990; MRR).

Investigating a sample of 15 protostellar jets including those above, MRR found that the flows are, in general, poorly collimated close to the source (within distances of roughly few 10^{-4} pc) and become highly collimated further out, on scales of the order of the jet lengths ($\sim 10^{-2}$–10^{-1} pc), showing a decrease in the jet opening angle with increasing distance. This clearly suggests that a large-scale collimation mechanism, probably due to the external environment is at work (MRR). The Haro 6-5B and HH 24G jets, in particular, narrow with increasing distance from the source, like the jets of Figures 2*a* and 2*b*.

The Haro 6-5B northern jet extends over $L_j \simeq 0.1$ pc, and its source is surrounded by an extended reflection nebula whose brightest part lies on the jet axis at $\sim 7 \times 10^{-3}$ pc. Within 10^{-3} pc of the source, the jet has a strong lateral expansion which is followed by a gap (between ~ 1 and 1.7×10^{-3} pc) where the jet is not seen. Further out, the jet is recollimated and *narrows* over most of its length. Its elongated structure is knotty and *wiggling*. After that, the jet becomes again invisible and then shows up in a distant bow-shaped nebula ($\simeq 0.1$ pc from the source). As suggested by MRR, the initial expansion is likely to be a signature of a highly overpressured and poorly collimated flow. The appearance of the jet outside 1.7×10^{-3} pc, where the expansion is slow ($\Delta R/\Delta x \sim 0.025$), is reminiscent of the jet brightening and collimation that we see in simulations of cooling jets in an ambient medium of increasing density (Figs. 2*a* and 2*b*). K-H instabilities here would drive

the formation of internal shocks and small amplitude wiggles, so that the observed bright knots might be oblique internal shocks excited by the K-H modes (as seen in Fig. 2) instead of being due to intermittent jet ejection (see, e.g., GB94). Outside this part of the flow, the disappearance of the jet might arise from passage through an ambient medium with decreasing density (and pressure), which would lead to a low emissivity (as in Fig. 1*c*). The distant bow-shaped nebula could mark an impact between the jet and a last dense part of the ambient medium (see, e.g., GB93), or it could be a relic of a much earlier outflow episode in a more homogeneous ambient medium (see, e.g., GB94). The morphology of the Haro 6-5B counterjet is radically different from that of the jet, suggesting that intrinsic asymmetries due to environmental effects are at work (MRR).

Since we did not choose parameters for our simulations to fit the particular case of the Haro 6-5B jet, our results can provide only qualitative descriptions of the observations. Nonetheless, we can estimate the changes in the flow parameters that would be required to produce the observed expansion and collimation of the Haro 6-5B jet. The collimated part of the jet flow has and expansion rate $(\Delta R/\Delta x)_{\rm obs} \simeq 0.025$ (MRR), and in our simulations of the $\eta = 3$ jet propagating into an increasing pressure environment (Figs. 1*a* and 2*b*) we find $\Delta R/\Delta x \sim 2$ times smaller. This suggests that a reduction of the jet overpressure by a factor $\sim$4 would cause a better match between our simulations and the observed flow. We note that the ambient temperature used in our simulations (and thus p_a) is somewhat larger than the observed values in star forming regions, an approximation that has been used in previous work (see, e.g., BFK, GB93, GB94) partially to mimic the presence of a magnetic pressure. A decrease of T_a in our simulations would be consistent, for example, with the required decrease of p_a in order to fit the observed expansion and narrowing of the Haro 6-5B jet.

Large-amplitude side-to-side wiggles and knots are also observed in HH 30, HH 83, HH 84, HH 85, HH 110, and other jet systems (see, e.g., MRR; Reipurth 1989). Such features could also be due to the mechanism discussed here. We note, however, that some of these jets keep broadening slowly with distance (e.g., HH 30) or have an approximately constant width over a section of their length (e.g., HH 83). This would suggest less efficient confinement by the ambient medium in these cases, perhaps because of a larger initial density ratio between jet and ambient gas, as in the high η jet of Figure 2*c*, or a smoother density stratification of the ambient medium (smaller α; see eq. [1]).

Although, on average, the jets of Figure 2 are decelerated by the increasing ram pressure of the ambient medium, we find that the velocity of advance of their working surfaces, $v_{\rm ws}$, has an oscillating pattern. Since the density ratio η decreases with distance, $v_{\rm ws} \simeq v_j/[1 + (\eta\epsilon)^{-1/2}]$ (see, e.g., eq. [1] of GB93) initially decreases as the jet propagates downstream with a ratio of jet to head square radius $\epsilon \equiv (R_j/R_h)^2 \simeq 1$. Later, as the jet head is compressed by the ambient medium, the increase of ϵ more than compensates for the decrease of η, and the jet head accelerates as it narrows. Eventually, the further decrease of η dominates the equation and the working surface decelerates again. For example, the $\eta(x_0) = 3$ jet of Figure 2*b* follows the $v_{\rm ws}(\epsilon)$ relation above within $\sim$30%. The internal shocks of Figure 2 are regularly spaced (at $\sim$1 to 2 R_j) and travel downstream with a similar variable velocity pattern. Their speed gets closer to $v_{\rm ws}$ as they approach the jet head. Recent measurements of the tangential velocity of the knots of Haro 6-5B (Eislöffel 1993) indicate an oscillating pattern in qualitative agreement with the results above. Further measurements of variations of the proper motions of knots in systems like HH 24G or HH 83 would be an interesting check on our predictions. It is also important to note that the variations of the shock velocity at the working surface imply variations in the intensity of emission from the associated cooling regions behind the shocks.

We are indebted to the referees (Colin Masson and an anonymous referee) and to Tom Ray for their fruitful suggestions. Also E. M. d. G. D. P. is thankful to R. Mundt for his kind hospitality during the Workshop on Disk and Outflows from Young Stars at the Max-Planck-Institut in Heidelberg and his relevant and fruitful comments on this work. The simulations were performed on HP Apollo 9000/720 and DEC 3000/600 AXP Workstations whose purchase was made possible by the Brazilian Agency FAPESP. This work has been partially supported by the Brazilian Agency CNPq.

REFERENCES

Bally, J., & Devine, D. 1994, ApJ, 428, L65
Birkinshaw, M. 1991, in Beams and Jets in Astrophysics, ed. P. A. Hughes (Cambridge: Cambridge Univ. Press), 278
Blondin, J. M., Fryxell, B. A., & Königl, A. 1990, ApJ, 360, 370 (BFK)
Chernin, L., Masson, C., de Gouveia Dal Pino, E. M., & Benz, W. 1994, ApJ, 426, 204 (CMGB)
de Gouveia Dal Pino, E. M., & Benz, W. 1993, ApJ, 410, 686 (GB93)
———. 1994, ApJ, 435, 261 (GB94)
de Gouveia Dal Pino, E. M., & Birkinshaw, M. 1996, in preparation (GB96)
Eislöffel, J. 1993, Ph.D. thesis, Univ. Heidelberg
Fuller, G. A., & Myers, P. C. 1992, ApJ, 384, 523
Hardee, P. E., et al. 1992, ApJ, 387, 460
Hartigan, P., Mundt, R., & Stocke, J. 1986, AJ, 91, 1357
Hartigan, P., & Raymond, J. 1992, ApJ, 409, 705
Katz, J. 1989, Ph.D. thesis, Princeton Univ.
Massaglia, S., et al. 1995, A&A, submitted
Mundt, R., et al. 1990, A&A, 232, 37
Mundt, R., Brugel, E. W., & Bührke, T. 1987, ApJ, 319, 275
Mundt, R., Ray, T. P., & Raga, A. C. 1991, A&A, 252, 740 (MRR)
Raga, A. C., & Kofman, L. 1992, ApJ, 386, 222
Reipurth, B. 1989, in Proc. ESO Workshop on Low Mass Star Formation and Pre-Main Sequence Objects, ed. B. Reipurth (Garching: ESO), 247
Stone, J. M., & Norman, M. L. 1993, ApJ, 413, 198
———. 1994, ApJ, 420, 237
Wiita, P. J., Rosen, A., & Norman, M. L. 1990, ApJ, 350, 545